Direct assessment of vorticity alignment with local and nonlocal strain rates in turbulent flows

Peter E. Hamlington,[1] Jörg Schumacher,[2] and Werner J. A. Dahm[1]
[1]*Laboratory for Turbulence and Combustion, Department of Aerospace Engineering, The University of Michigan, Ann Arbor, Michigan 48109-2140, USA*
[2]*Institute for Thermodynamics and Fluid Mechanics, Technische Universität Ilmenau, D-98684 Ilmenau, Germany*

(Received 6 August 2008; accepted 18 September 2008; published online 19 November 2008)

A direct Biot-Savart integration is used to decompose the strain rate into its local and nonlocal constituents, allowing the vorticity alignment with the local and nonlocal strain rate eigenvectors to be investigated. These strain rate tensor constituents are evaluated in a turbulent flow using data from highly resolved direct numerical simulations. While the vorticity aligns preferentially with the intermediate eigenvector of the *combined* strain rate, as has been observed previously, the present results, for the first time, clearly show that the vorticity aligns with the most extensional eigenvector of the *nonlocal* strain rate. This, in turn, reveals a significant linear contribution to the vortex stretching dynamics in turbulent flows. © *2008 American Institute of Physics*.
[DOI: 10.1063/1.3021055]

The alignment of vorticity with the strain rate eigenvectors in turbulent flows has been a subject of considerable interest over the past two decades. Since the initial finding[1] that the vorticity shows a preferred alignment with the intermediate eigenvector of the strain rate tensor, there have been numerous studies seeking to understand the reasons for this result, and various theoretical approaches have been proposed to explain the failure of the vorticity to align with the most extensional strain rate eigenvector.

In this letter, we help resolve this issue by showing that vorticity in turbulence does tend toward alignment with the most extensional eigenvector of the *nonlocal* (background) strain, namely, the strain field induced in the immediate region around any vortical structure by the surrounding vorticity outside this region. The anomalous alignment occurs with the eigenvectors of the *combined* strain rate, namely, the sum of this nonlocal background strain and the *local* strain induced in the region by the vorticity within it.

Alignment of the vorticity vector $\boldsymbol{\omega} \equiv \nabla \times \mathbf{u}$ with the strain rate tensor S_{ij} in three-dimensional incompressible turbulent flows is ultimately responsible for the transfer of kinetic energy between scales, and for the nonlinearity in the dynamics of the underlying vorticity field. The inverse curl operator is the Biot-Savart integral that gives the velocity field $\mathbf{u}$ from the vorticity field $\boldsymbol{\omega}$ as

$$\mathbf{u}(\mathbf{x}) = \frac{1}{4\pi}\int_{\mathbf{x}'} \boldsymbol{\omega}(\mathbf{x}') \times \frac{\mathbf{x}-\mathbf{x}'}{|\mathbf{x}-\mathbf{x}'|^3} d^3\mathbf{x}'. \tag{1}$$

The resulting gradients of $\mathbf{u}$ define the strain rate tensor $S_{ij} = \frac{1}{2}(\partial u_i/\partial x_j + \partial u_j/\partial x_i)$ which, in turn, is coupled to the dynamics of the vorticity as

$$\frac{D\omega_i}{Dt} = S_{ij}\omega_j + \nu\nabla^2\omega_i. \tag{2}$$

On the right side of Eq. (2), the magnitude of the stretching term $|S_{ij}\omega_j| \equiv \omega[s_i^2(\mathbf{e}_i \cdot \mathbf{e}_\omega)^2]^{1/2}$ depends on the strain rate eigenvalues s_i and the vorticity magnitude $\omega \equiv (\omega_i\omega_i)^{1/2}$, and on the alignment cosines $(\mathbf{e}_i \cdot \mathbf{e}_\omega)$ between the vorticity unit vector $\mathbf{e}_\omega$ and the strain rate eigenvectors $\mathbf{e}_i$.

The three strain rate eigenvalues s_i can be ordered as $s_1 \geq s_2 \geq s_3$ so that incompressibility $(s_1+s_2+s_3 \equiv 0)$ requires $s_1 \geq 0$ and $s_3 \leq 0$. The positivity of s_1 and the negativity of s_3 correspond, respectively, to extensional and compressional straining along the $\mathbf{e}_1$ and $\mathbf{e}_3$ directions. While the intermediate eigenvalue s_2 is on average weakly positive in turbulent flows, the instantaneous s_2 can take on large positive or negative values[1–3] bounded only by the s_1 and s_3 values. The alignment between the vorticity and the strain rate eigenvectors similarly determines the production rate $\omega_i S_{ij} \omega_j \equiv \omega^2 s_i (\mathbf{e}_i \cdot \mathbf{e}_\omega)^2$ for the enstrophy $\frac{1}{2}(\boldsymbol{\omega} \cdot \boldsymbol{\omega})$. The three alignment cosines $(\mathbf{e}_i \cdot \mathbf{e}_\omega)$ thus play an essential role in the structure and dynamics of turbulent flows.

Despite its importance, the mechanism by which the vorticity aligns with the strain rate eigenvectors $\mathbf{e}_i$ is still not well understood. In particular, the maximality and positivity of s_1 might suggest that the vorticity in Eq. (2) would show preferred alignment with the most extensional eigenvector $\mathbf{e}_1$. However, since S_{ij} on the right side of Eq. (2) is coupled back to ω_i, the resulting nonlinearity complicates any such simple alignment. Indeed, numerous studies have shown that the vorticity in turbulent flows instead shows a preference for alignment with the intermediate strain rate eigenvector $\mathbf{e}_2$.

This can be seen, for example, in Fig. 1, where distributions of the three alignment cosines $|\mathbf{e}_i \cdot \mathbf{e}_\omega|$ are shown from a recent highly resolved, three-dimensional, 2048^3 direct numerical simulation[4] (DNS) of statistically stationary, forced, homogeneous, isotropic turbulence at Taylor-scale Reynolds number $\mathrm{Re}_\lambda = 107$. The simulation was done using a pseudospectral method with a spectral resolution that exceeds the standard value by a factor of 8. As a result the highest wavenumber corresponds to $k_{\max}\eta_K = 10$, and the Kolmogorov length scale η_K is resolved with three grid spacings. The

 © 2008 American Institute of Physics

Downloaded 19 Nov 2008 to 141.212.190.118. Redistribution subject to AIP license or copyright; see http://pof.aip.org/pof/copyright.jsp

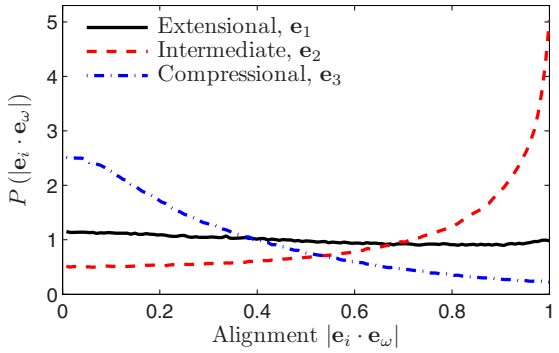

FIG. 1. (Color online) Distributions of alignment cosines $|\mathbf{e}_i \cdot \mathbf{e}_\omega|$.

resulting alignment distributions in Fig. 1 agree with those from lower-resolution DNS studies as well as from laboratory measurements.[3,5,6] In particular, the vorticity tends to point away from the most compressive eigenvector $\mathbf{e}_3$, namely, $|\mathbf{e}_3 \cdot \mathbf{e}_\omega| \to 0$, and there is essentially no tendency for any preferred alignment relative to the most extensional strain rate eigenvector $\mathbf{e}_1$ since $P(|\mathbf{e}_1 \cdot \mathbf{e}_\omega|) \approx 1$. However, the vorticity shows a strong tendency toward alignment with the intermediate strain rate eigenvector $\mathbf{e}_2$, namely, $|\mathbf{e}_2 \cdot \mathbf{e}_\omega| \to 1$.

Previous attempts to understand these alignments have often focused on the vorticity-strain coupling in the evolution equation for the strain rate tensor, namely,

$$\frac{DS_{ij}}{Dt} = -S_{ik}S_{kj} - \frac{1}{4}(\omega_i\omega_j - \omega_k\omega_k\delta_{ij}) - \frac{1}{\rho}\Pi_{ij} + \nu\nabla^2 S_{ij}, \quad (3)$$

where $\Pi_{ij} \equiv \partial^2 p / \partial x_i \partial x_j$ is the pressure Hessian. The nonlinear coupling between the strain rate and the vorticity is apparent in Eqs. (2) and (3), where the nonlocality of the vorticity and strain rate coevolution involves the pressure Hessian.[7,8] While progress has been made in understanding the vorticity alignments in Fig. 1 via the restricted Euler equations (e.g., Ref. 8), where nonlocal effects are neglected entirely, a complete picture that clearly distinguishes between local and nonlocal contributions to the vorticity dynamics has remained largely elusive.

Here, we forgo the use of Eq. (3) in representing the strain rate appearing in Eq. (2), instead using an integral representation for the strain rate derived from Eq. (1), and then use this to gain insights into the effects of nonlocality and nonlinearity on the vorticity alignment. As shown in Ref. 9, from the Biot-Savart integral in Eq. (1) the strain rate can be exactly expressed in terms of the vorticity as

$$S_{ij}(\mathbf{x}) = \frac{3}{8\pi}\int_{\mathbf{x}'} (\epsilon_{ikl}r_j + r_i\epsilon_{jkl})\frac{r_k}{r^5}\omega_l(\mathbf{x}')d^3\mathbf{x}', \quad (4)$$

where $\mathbf{r} \equiv \mathbf{x} - \mathbf{x}'$, $r \equiv |\mathbf{r}|$, and the integral is defined in a principal value sense. Substituting Eq. (4) in Eq. (2) then gives a direct nonlocal integro-differential equation for the vorticity evolution as

$$\frac{D\omega_i}{Dt} = \frac{3}{8\pi}\int_{\mathbf{x}'} (\epsilon_{ikl}r_j + r_i\epsilon_{jkl})\frac{r_k}{r^5}[\omega_j(\mathbf{x})\omega_l(\mathbf{x}')]d^3\mathbf{x}' + \nu\nabla^2\omega_i, \quad (5)$$

which depends only on the vorticity field itself. In Eqs. (4) and (5), the local and nonlocal contributions to the strain rate and vorticity dynamics can be understood by separating the integration domain into a local region of radius $r \le R$ centered on $\mathbf{x}$, and a nonlocal region that accounts for the rest of the domain.[9,10] The strain rate in Eq. (4) then is the sum

$$S_{ij}(\mathbf{x}) = S_{ij}^R(\mathbf{x}) + S_{ij}^B(\mathbf{x}) \quad (6)$$

of the local strain rate $S_{ij}^R(\mathbf{x})$ induced at $\mathbf{x}$ by the vorticity within R, and the nonlocal (background) strain rate $S_{ij}^B(\mathbf{x})$ induced at $\mathbf{x}$ by all the vorticity outside R.

The background strain field $S_{ij}^B(\mathbf{x})$ in the vicinity of any local vortical structure in the turbulence is that induced by all the *other* vortical structures. Thus, the proper physical value for R used to obtain $S_{ij}^B(\mathbf{x})$ should exclude from Eq. (4) essentially all the vorticity associated with any local vortical structure. Prior studies (e.g., Ref. 11) have shown that the characteristic radius of intense vortical structures in turbulence is in the range $r/\eta_K \approx 4-10$, where η_K is the Kolmogorov length scale. This is consistent with the two-point vorticity correlation from the present DNS of homogeneous isotropic turbulence, which is found to decrease to 20% of its maximum value at $r \approx 12\eta_K$. This gives a physically appropriate cutoff radius since beyond this the vorticity becomes essentially uncorrelated with itself. Thus, $R = 12\eta_K$ as used herein excludes essentially all the local vorticity for most structures, and thereby allows the self-induced strain field in the vicinity of typical vortical structures to be separated from the background strain field in which the structures reside.

Although Ref. 9 developed an operator for the background strain rate $S_{ij}^B(\mathbf{x})$, here we avoid the associated infinite Taylor series with respect to R and instead obtain the local strain rate $S_{ij}^R(\mathbf{x})$ by directly integrating Eq. (4) over the domain R centered on $\mathbf{x}$. At any point $\mathbf{x}$ in the 2048^3 cubic simulation domain, a smaller cubic subdomain with side length $2R$ is taken to define the local region around $\mathbf{x}$. The local strain rate $S_{ij}^R(\mathbf{x})$ is obtained by numerically integrating Eq. (4) over this subdomain. We then determine the nonlocal strain rate from Eq. (6) as $S_{ij}^B(\mathbf{x}) = S_{ij}(\mathbf{x}) - S_{ij}^R(\mathbf{x})$, and examine the alignment of the vorticity $\boldsymbol{\omega}(\mathbf{x})$ with each of these strain rates to understand how the alignment in Fig. 1 arises.

Figure 2 shows an example of the resulting decomposition of the shear strain rate field $S_{12}(\mathbf{x})$ into its background and local fields, $S_{12}^B(\mathbf{x})$ and $S_{12}^R(\mathbf{x})$. Similar local-nonlocal decompositions are obtained for the other strain rate components, and the eigenvalues and eigenvectors of the resulting background and local strain rate tensor fields are then computed. At every point $\mathbf{x}$, the alignment cosines $|\mathbf{e}_i \cdot \mathbf{e}_\omega|$ of the vorticity with the background and local strain rate eigenvectors, denoted $\mathbf{e}_i^B$ and $\mathbf{e}_i^R$, respectively, are then evaluated.

The resulting vorticity alignment distributions $P(|\mathbf{e}_i^B \cdot \mathbf{e}_\omega|)$ and $P(|\mathbf{e}_i^R \cdot \mathbf{e}_\omega|)$ are shown in Figs. 3(a) and 3(b), respectively. From the *background* strain alignments in Fig. 3(a), it is apparent that the vorticity is preferentially aligned with the most *extensional* background strain rate eigenvector $\mathbf{e}_1^B$,

Downloaded 19 Nov 2008 to 141.212.190.118. Redistribution subject to AIP license or copyright; see http://pof.aip.org/pof/copyright.jsp

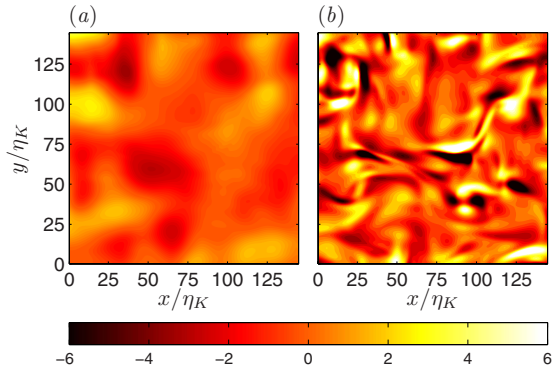

FIG. 2. (Color online) Typical example of (a) background strain rate field $S_{12}^B(\mathbf{x})$ and (b) local strain rate field $S_{12}^R(\mathbf{x})$.

namely, $|\mathbf{e}_1^B \cdot \mathbf{e}_\omega| \to 1$. There is essentially no preferred alignment of the vorticity relative to the intermediate background eigenvector $\mathbf{e}_2^B$ since $P(|\mathbf{e}_2^B \cdot \mathbf{e}_\omega|) \approx 1$, while the vorticity tends to point preferentially away from the most compressive background eigenvector $\mathbf{e}_3^B$, namely, $|\mathbf{e}_3^B \cdot \mathbf{e}_\omega| \to 0$.

The alignments in Fig. 3(a) with the background strain rate are precisely as would be expected when the strain rate evolution is decoupled from that of the vorticity, as is essentially the case for the background strain. From Eq. (2) with Eq. (6), the inviscid dynamics of the vorticity satisfies

$$\frac{D\omega_i}{Dt} = S_{ij}^B \omega_j + S_{ij}^R \omega_j. \tag{7}$$

By definition, the background strain rate S_{ij}^B in Eq. (7) is independent of the vorticity at $\mathbf{x}$, and thus its effect on the dynamics of the vorticity $\omega_i(\mathbf{x})$ is essentially linear. Since $s_1^B \geq 0$ and $s_3^B \leq 0$, and since $s_2^B \leq s_1^B$, the effect is to cause $\boldsymbol{\omega}$ to rotate toward alignment with the most extensional eigenvector $\mathbf{e}_1^B$ of S_{ij}^B. The fact that such alignment of the vorticity is seen in Fig. 3(a) suggests that the quasilinear dynamics from the first term on the right in Eq. (7) plays at least a significant role in the overall evolution of the vorticity field in turbulent flows. In the terminology of She *et al.*,[10] this would be referred to as *kinematic nonlocality*, as distinguished from the *dynamic locality* that was the focus of their study.

From the vorticity alignments in Fig. 3(b) with the local strain rate field induced in R by the local vorticity, $\boldsymbol{\omega}$ shows substantial and essentially equal preference for pointing largely perpendicular to the most extensional and compressional eigenvectors $\mathbf{e}_1^R$ and $\mathbf{e}_3^R$ of the local strain rate S_{ij}^R, namely, $|\mathbf{e}_1^R \cdot \mathbf{e}_\omega| \to 0$ and $|\mathbf{e}_3^R \cdot \mathbf{e}_\omega| \to 0$. This is consistent with the fact that much of the vorticity in turbulent flows concentrates into relatively compact linelike and sheetlike structures formed by locally axisymmetric and planar background strain rate fields.[12,13] In the former case, the axisymmetric Burgers vortex is often used as an idealized representation of such structures, while in the latter case the planar Burgers vortex sheet provides a similar idealized representation. In both cases, the two-dimensional local strain field induced by the vortical structure has large extensional and compressional eigenvalues with eigenvectors that are necessarily perpendicular to the vorticity, due to the geometry of the structures. The remaining eigenvalue is zero for perfectly two-dimensional structures, and will be nonzero only due to small departures from strict two-dimensionality of the structures. Its small magnitude is thus nearly always between the other two eigenvalues, and will therefore be the intermediate eigenvalue. Its eigenvector must necessarily be perpendicular to the other two, and so will necessarily be closely aligned with the vorticity itself.

This is precisely the alignment seen with $\mathbf{e}_2^R$ in Fig. 3(b), where the vorticity points strongly along the direction of the intermediate eigenvector, namely $|\mathbf{e}_2^R \cdot \mathbf{e}_\omega| \to 1$. Note that this "preferred" alignment of the vorticity with the intermediate local strain eigenvector in Fig. 3(b) is not a result of the nonlinear dynamics from the second term on the right side in Eq. (7), but rather is a simple geometric consequence of the largely sheetlike and linelike structures into which the vorticity is formed.[12]

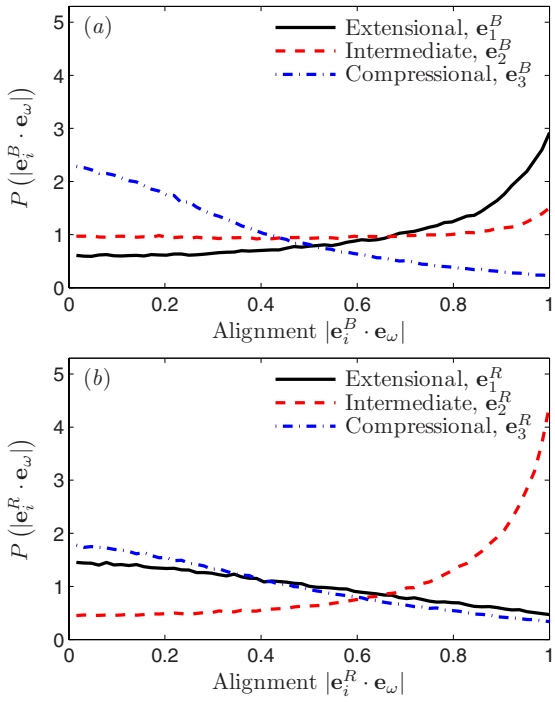

FIG. 3. (Color online) Distributions of vorticity alignment cosines for (a) background strain rate eigenvectors $\mathbf{e}_i^B$ and (b) local strain rate eigenvectors $\mathbf{e}_i^R$.

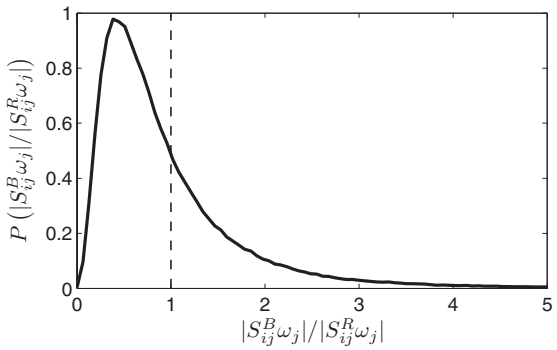

FIG. 4. Distribution of background (linear) to local (nonlinear) vortex stretching ratio.

Downloaded 19 Nov 2008 to 141.212.190.118. Redistribution subject to AIP license or copyright; see http://pof.aip.org/pof/copyright.jsp

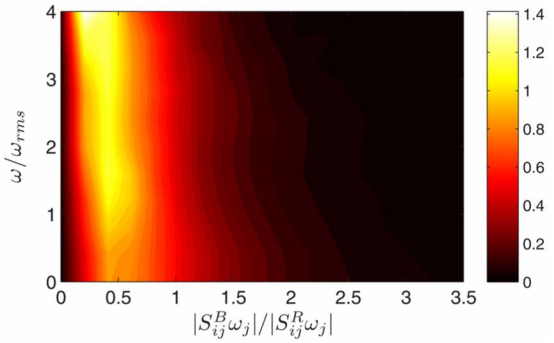

FIG. 5. (Color online) Distribution of background to local vortex stretching ratio conditioned on vorticity magnitude $\omega/\omega_{\mathrm{rms}}$.

The alignments in Fig. 3 allow the relative contributions from the two terms on the right side of the inviscid vorticity dynamics in Eq. (7) to be understood. In particular, Fig. 4 shows the distribution of the ratio of background and local vortex stretching rates, namely, $|S^B_{ij}\omega_j|/|S^R_{ij}\omega_j|$. It is apparent that in much of the flow this stretching ratio exceeds one, meaning that the linear stretching dynamics produced by the background (nonlocal) strain field S^B_{ij} in Eq. (7) exceeds the nonlinear stretching dynamics from the local strain field S^R_{ij}. Thus, despite the overall nonlinear dynamics governing the vorticity evolution in Eq. (2), a substantial part of the underlying dynamics is linear and nonlocal.

This is consistent with the alignment in Fig. 3(b) of the vorticity with the intermediate eigenvector of the local strain rate S^R_{ij}, for which the associated eigenvalue s^R_2 has the smallest magnitude among the three local strain eigenvalues, and thus the associated stretching is not necessarily large. By contrast, Fig. 3(a) shows that the vorticity aligns with the most extensional eigenvector of the background strain rate S^B_{ij}, and thus is stretched by the largest of its three eigenvalues. As a result, even when $|S^B_{ij}|$ is smaller than $|S^R_{ij}|$, the background stretching may be larger than the local stretching. This is a consequence of the fact that in Eq. (7) vortex stretching by the local strain rate is generally not favored from the standpoint of geometrical alignment. It is remarkable that the linear stretching dynamics from this background (nonlocal) strain field is comparable to the nonlinear stretching dynamics from the local strain field.

Further insights into the background and local dynamics may be gained by conditioning the vortex stretching ratio on the vorticity magnitude ω, as shown in Fig. 5. While there is a tendency toward smaller vortex stretching ratios for large vorticity magnitudes in Fig. 5, the observed dependence is relatively weak. This is due to the competition between increased local strain rate magnitude (which favors local stretching) and the correspondence with nearly two-dimensional intense vortical structures (which favors background stretching) for large values of ω. Unraveling the individual contributions of these two effects, as well as consideration of other secondary parameters such as the background strain persistence or the Reynolds number, is an important direction for future research.

P.E.H. and W.J.A.D. acknowledge support from the Air Force Research Laboratory (AFRL) through the Michigan-AFRL Collaborative Center for Aeronautical Sciences (MACCAS) under Award No. FA8650-06-2-3625, and by the National Aeronautics & Space Administration (NASA) Marshall and Glenn Research Centers under the NASA Constellation University Institutes Project (CUIP) under Grant No. NCC3-989. J.S. acknowledges support by the German Academic Exchange Service (DAAD) and the Heisenberg Program of the Deutsche Forschungsgemeinschaft (DFG). The simulations have been carried out at the Jülich Supercomputing Centre (Germany) within the Deep Computing Initiative of the DEISA Consortium.

[1] Wm. T. Ashurst, A. R. Kerstein, R. M. Kerr, and C. H. Gibson, "Alignment of vorticity and scalar gradient with strain rate in simulated Navier–Stokes turbulence," Phys. Fluids **30**, 2343 (1987).
[2] A. Tsinober, *An Informal Introduction to Turbulence* (Kluwer, Dordrecht, 2001).
[3] L. K. Su and W. J. A. Dahm, "Scalar imaging velocimetry measurements of the velocity gradient tensor field in turbulent flows. II. Experimental results," Phys. Fluids **8**, 1883 (1996).
[4] J. Schumacher, K. R. Sreenivasan, and V. Yakhot, "Asymptotic exponents from low-Reynolds-number flows," New J. Phys. **9**, 89 (2007).
[5] J. A. Mullin and W. J. A. Dahm, "Dual-plane stereo particle image velocimetry measurements of velocity gradient tensor fields in turbulent shear flow. II. Experimental results," Phys. Fluids **18**, 035102 (2006).
[6] A. Tsinober, E. Kit, and T. Dracos, "Experimental investigation of the field of velocity gradients in turbulent flows," J. Fluid Mech. **242**, 169 (1992).
[7] K. Ohkitani and S. Kishiba, "Nonlocal nature of vortex stretching in an inviscid fluid," Phys. Fluids **7**, 411 (1995).
[8] K. K. Nomura and G. K. Post, "The structure and dynamics of vorticity and rate of strain in incompressible homogeneous turbulence," J. Fluid Mech. **377**, 65 (1998).
[9] P. E. Hamlington, J. Schumacher, and W. J. A. Dahm, "Local and nonlocal strain rate fields and vorticity alignment in turbulent flows," Phys. Rev. E **77**, 026303 (2008).
[10] Z. S. She, E. Jackson, and S. A. Orszag, "Structure and dynamics of homogeneous turbulence: Models and simulations," Proc. R. Soc. London, Ser. A **434**, 101 (1991).
[11] J. Jimenez, A. A. Wray, P. G. Saffman, and R. S. Rogallo, "The structure of intense vorticity in isotropic turbulence," J. Fluid Mech. **255**, 65 (1993).
[12] J. Jimenez, "Kinematic alignment effects in turbulent flows," Phys. Fluids A **4**, 652 (1992).
[13] K. A. Buch and W. J. A. Dahm, "Experimental study of the fine-scale structure of conserved scalar mixing in turbulent shear flows. Part 1. Sc $\gg$1," J. Fluid Mech. **317**, 21 (1996).

Downloaded 19 Nov 2008 to 141.212.190.118. Redistribution subject to AIP license or copyright; see http://pof.aip.org/pof/copyright.jsp